◆ Human Brain Mapping 28:118–133(2007) ◆

Intelligence and EEG Current Density Using Low-Resolution Electromagnetic Tomography (LORETA)

R.W. Thatcher,[1,2]* D. North,[1] and C. Biver[1]

[1]*EEG and NeuroImaging Laboratory, Bay Pines VA Medical Center, St. Petersburg, Florida*
[2]*Department of Neurology, University of South Florida College of Medicine, Tampa, Florida*

Abstract: The purpose of this study was to compare EEG current source densities in high IQ subjects vs. low IQ subjects. Resting eyes closed EEG was recorded from 19 scalp locations with a linked ears reference from 442 subjects ages 5 to 52 years. The Wechsler Intelligence Test was administered and subjects were divided into low IQ (≤90), middle IQ (>90 to <120) and high IQ (≥120) groups. Low-resolution electromagnetic tomographic current densities (LORETA) from 2,394 cortical gray matter voxels were computed from 1–30 Hz based on each subject's EEG. Differences in current densities using *t* tests, multivariate analyses of covariance, and regression analyses were used to evaluate the relationships between IQ and current density in Brodmann area groupings of cortical gray matter voxels. Frontal, temporal, parietal, and occipital regions of interest (ROIs) consistently exhibited a direct relationship between LORETA current density and IQ. Maximal *t* test differences were present at 4 Hz, 9 Hz, 13 Hz, 18 Hz, and 30 Hz with different anatomical regions showing different maxima. Linear regression fits from low to high IQ groups were statistically significant ($P < 0.0001$). Intelligence is directly related to a general level of arousal and to the synchrony of neural populations driven by thalamo-cortical resonances. A traveling frame model of sequential microstates is hypothesized to explain the results. *Hum Brain Mapp 28: 118–133, 2007.*

Key words: qEEG; intelligence; neuropsychological tests; LORETA current density; neuroimaging

INTRODUCTION

Previous studies from this laboratory used discriminant analyses and multivariate regression to investigate the relationship between intelligence and the scalp surface EEG [Thatcher et al., 2005]. Two interrelated categories of measurement were studied: 1–19 channels of scalp recorded EEG power and 2–171 EEG electrode combinations of the 19 channels of EEG coherence, phase, and amplitude asymmetry. The study found that the statistical effect size of the correlation between EEG and IQ was rank ordered as: EEG phase > EEG coherence > EEG amplitude asymmetry > absolute power > relative power and power ratios [Thatcher et al., 2005]. The strongest correlations to IQ were short EEG phase delays in the frontal lobes and long phase delays in the posterior cortical regions as well as reduced EEG coherence. Specific frequency bands were analyzed with the alpha and beta bands the strongest for absolute power, while coherence and phase were essentially independent of frequency. For example, the distribution of statistically significant absolute power values was greatest in the alpha band (8–12 Hz, 33.2%), the delta (1–3.5 Hz, 30.2%), and the beta band (13–22 Hz, 27.8%). The theta band (4–7 Hz, 8.8%) exhibited the weakest effect size [Thatcher et al., 2005].

The frequency findings in the Thatcher et al. [2005] study are similar to EEG power studies that show medium to

*Correspondence to: Robert W. Thatcher, Ph.D., NeuroImaging Laboratory, Research and Development Service – 151, Veterans Administration Medical Center, Bay Pines, FL 33744.
E-mail: rwthatcher@yahoo.com

Received for publication 19 October 2005; Accepted 4 February 2006
DOI: 10.1002/hbm.20260
Published online 25 May 2006 in Wiley InterScience (www.interscience.wiley.com).

TABLE I. Number of subjects in different IQ groups and ages

IQ groups	N	Full IQ range	Mean age	StDev Age	Age range
Low IQ	80	71-90	11.78	5.49	5.00-52
Middle IQ	259	91-119	10.99	3.75	5.00-39
High IQ	97	120-154	10.41	4.66	5.17-37

strong effect size at specific resonant frequencies in correlations to IQ [Gasser et al., 1983; Giannitrapani, 1985; Marosi et al., 1999; Schmid et al., 2002; Thatcher et al., 1998, 2001]. Schmid et al. [2002] found significant differences between IQ groups at 0.5–1.5 Hz and 3.0–5 Hz, with the highest statistical significance at 9 Hz. In contrast, Marosi et al. [1999] reported a broader range of frequencies related to intelligence. Low-resolution electromagnetic tomography (LORETA) of changes in full width at half maximum (FWHM) of the spatial spread of currents and increased 3D current density have also been positively related to IQ [Jausovec and Jausovec, 2001, 2003].

Frequency resonance is a fundamental property of the EEG [Nunez, 1981, 1994] and the experimental design in the Thatcher et al. [2005] study of coherence and phase involved relatively large frequency bands and did not investigate the power spectrum at a high frequency resolution. Therefore, the purpose of the present study was to investigate the differences in current density in high IQ vs. low IQ subjects using LORETA with an emphasis on the spectrum from 1–30 Hz at 1 Hz resolution. Of particular interest are differences in LORETA current density in high and low IQ subjects in different 3D cortical regions of interest (ROIs) as well as left vs. right hemispheres in the frequency range of 1–30 Hz.

SUBJECTS AND METHODS

Subjects

The study involved the same subjects as in Thatcher et al. [2005] and included a total of 442 subjects ranging in age from 5 to 52.75 years (male, n = 260). The age distribution was weighted toward younger subjects, with n = 392 in the age range 5 to 15, n = 40 in the age range 16 to 25, and n = 4 in the age range 26 to 55. However, age was not a confounding variable because there were no statistically significant differences in age between different IQ groups. Subjects with a history of neurological disorders were excluded from the study and none of the subjects had taken medication less than 24 hours before testing. The subjects were divided into three groups: 1, low IQ (full-scale IQ 70–90, n = 80); 2, mid-range IQ (full-scale IQ 91–119, n = 259); and 3, a high IQ group (full-scale IQ = 120, n = 97). The demographics and full-scale IQ means, ranges, and standard deviations of the three groups of subjects are shown in Table I.

Neuropsychological Measures

Neuropsychological and school achievement tests were administered on the same day that the EEG was recorded. The order of EEG and neuropsychological testing was randomized and counterbalanced so that EEG was measured before neuropsychological tests in one-half of the subjects and neuropsychological tests were administered before the EEG in the other half of the subjects. All testing was performed on the same day. The Wechsler Intelligence Scale for Children revised (WISC-R) was administered for individuals between 5 and 16 years and the Wechsler Adult Intelligence Scale revised (WAIS-R) was administered to subjects older than 16 years. The neuropsychological subtests for estimating full-scale IQ were equivalent for the WISC-R and the WAIS and included information, mathematics, vocabulary, block design, digit span, picture completion, coding, and mazes.

EEG Recording

The EEG was recorded from 19 scalp locations based on the International 10/20 system of electrode placement, using linked ears as a reference. University of Maryland-built EEG amplifiers were used to acquire EEG from 380 of the subjects at a 100-Hz sample rate and Lexicor-NRS 24 EEG amplifiers at a 128-Hz sample rate were used to acquire EEG from 62 of the subjects. There were no significant differences in the distribution of IQ scores or in the age range of subjects acquired by the two amplifier systems and the frequency characteristics of the two amplifier systems were essentially identical. Both amplifier systems were 3 db down at 0.5 Hz and 30 Hz and the Lexicor NRS-24 Amplifiers and the University of Maryland amplifiers were calibrated and equated using sine wave calibration signals and standardized procedures. Two- to 5-minute segments of EEG were recorded during an eyes-closed resting condition for all subjects. Each EEG record was visually examined and then edited to remove artifact using the Neuroguide software program. Split-half reliability tests and test retest reliability tests were conducted on the edited EEG segments and only records with >90% reliability were entered into the spectral analyses.

Cross-Spectral Analysis and LORETA computation

The edited EEG was saved in which the 19 channels were columns and the 256 time points as rows. In order to minimize windowing effects, 75% overlapping 256 point segments were used according to the procedure described by Kaiser and Sterman [2001]. Cross-spectral analyses using the Hermitian matrix for LORETA implementation were computed according to standard procedures for LORETA frequency analyses [Frei et al., 2001; Gomez and Thatcher, 2001; Pascual-Marqui, 2003]. A cosine taper windowing was performed using the cross-spectral FFT on each 256 point data sample. The cross-spectra were averaged across the overlapping windows, which yielded a total of 61 frequencies from

TABLE II. Regions of interest (ROIs) and corresponding Brodmann groupings and lobule groupings of voxels (from Key Inst. Pascual-Marqui [2003])

REGIONS of INTEREST	Frontal-Brodmann Areas	Temporal-Brodmann Areas	Parietal-Brodmann Areas	Occipital-Brodmann Areas
Anterior Cingulate	25,24,32,33,10			
Extra-Nuclear	13,47			
Inferior Frontal Gyrus	9,10,11,44,45,46,47			
Medial Frontal Gyrus	6,8,9,10,11,25,46,47			
Middle Frontal Gyrus	6,8,9,10,11,46,47			
Orbital Gyrus	11,47			
Paracentral Lobule	5,6,31,4			
Precentral Gyrus	4,6,43,44			
Rectal Gyrus	11			
Subcallosal Gyrus	25,34,13			
Superior Frontal Gyrus	6,8,9,10,11			
Fusiform Gyrus		20,36,37		
Inferior Temporal Gyrus		20,21,37		
Insula		13		
Middle Temporal Gyrus		21,20,38,37,22,39		
Parahippocampal Gyrus		28,30,35,36,34		
Sub-Gyral		20,21,37,40,6		
Superior Temporal Gyrus		13,21,22,38,39,41,42		
Transverse Temporal Gyrus		41,42		
Uncus		20,28,36		
Angular Gyrus			39	
Cingulate Gyrus			23,24,31,32	
Inferior Parietal Lobule			7,39,40	
Postcentral Gyrus			1,2,3,5,7,40,43	
Posterior Cingulate			23,29,30,31	
Precuneus			7,19,31,39	
Superior Parietal Lobule			7	
Supramarginal Gyrus			40	
Cuneus				7,17,18,19,30
Inferior Occipital Gyrus				17,18,19
Lingual Gyrus				17,18,19
Middle Occipital Gyrus				18,19,37
Superior Occipital Gyrus				19

0.5–30 Hz. The spectral resolution was 0.5 Hz; however, adjacent frequency bands were averaged to produce a 1-Hz resolution, thus yielding a total of 30 frequency bands from 1–30 Hz. The Key Institute software was used to compute the T matrix according to the Talairach Atlas coordinates of the Montreal Neurological Institute's MRI average of 305 brains [Pascual-Marqui, 1999; 2003, Talairach and Tournoux, 1988]. The computations were restricted to the cortical gray matter according to digitized probability atlases [Mazziota et al., 1995]. The spatial resolution was 7 mm for each of the 2,394 gray matter voxels. The cross-spectral values at each 1-Hz frequency band were multiplied by the T matrix, which is a 3D matrix of x, y, and z current source moments in each of the 2,394 gray matter voxels. The resultant current source vector at each pixel was computed as the square root of the sum of the squares for the x, y, and z source moments for each 1-Hz frequency band for each subject. The log transform of the current density values was computed but similar statistical findings with nearly identical effect sizes were observed with or without log transform. Therefore, for simplicity only the untransformed current source vectors are used in the present study.

Regions of Interest

The anatomical names and Brodmann areas that correspond to each of the 2,394 gray matter voxels in Talairach atlas coordinates was provided by Lancaster et al. [2000] as used by the Key Institute software [Pascual-Marqui, 2003]. Only distance 1 was used, which is the best approximation of a given voxel to a given ROI in both Brodmann area values and by anatomical names. After computing the LORETA currents for each of the 2,394 gray matter voxels, the Key-Talairach table of gray matter voxels was sorted by anatomical name and an average current density for a given ROI was computed by summing the current values for each of the gray matter voxels in an ROI and then dividing by the number of voxels. This resulted in a total of 66 different averages of current density based on anatomical ROIs in which 33 were from the left hemisphere and 33 were from the right hemisphere. A second level of averaging involved averaging the current densities in the four general Brodmann lobules of frontal, temporal, parietal, and occipital, which yielded eight lobules of averaged current density: four left and four right hemisphere lobules. Table II shows the Brodmann areas associated with the four different lob-

TABLE III. Talairach Atlas coordinates for left and right hemisphere regions of interest

	Left hemisphere: *x*, *y*, *z*	Right hemisphere: *x*, *y*, *z*
Anatomical Regions		
Angular Gyrus	−47, −65, 32	46, −65, 34
Anterior Cingulate	−5, 29, 8	6, 30, 7
Cingulate Gyrus	−5, −13, 35	6, −11, 35
Cuneus	−9, −82, 17	9, −77, 19
Extra-Nuclear	−36, 10, −6	37, 12, −6
Fusiform Gyrus	−43, −43, −15	45, −41, −16
Inferior Frontal Gyrus	−40, 24, −1	42, 24, 1
Inferior Occipital Gyrus	−36, −81, −5	36, −84, −5
Inferior Parietal Lobule	−48, −42, 42	50, −42, 40
Inferior Temporal Gyrus	−52, −27, −20	53, −28, −19
Insula	−39, −8, 7	40, −6, 9
Lingual Gyrus	−11, −73, −1	12, −70, −1
Medial Frontal Gyrus	−6, 31, 19	6, 33, 16
Middle Frontal Gyrus	−35, 31, 24	36, 30, 26
Middle Occipital Gyrus	−38, −81, 7	40, −78, 9
Middle Temporal Gyrus	−54, −35, −2	53, −33, −3
Orbital Gyrus	−7, 50, −21	8, 43, −22
Paracentral Lobule	−5, −32, 55	6, −31, 53
Parahippocampal Gyrus	−25, −24, −12	25, −26, −10
Postcentral Gyrus	−49, −25, 38	48, −26, 41
Posterior Cingulate	−9, −57, 15	10, −55, 15
Precentral Gyrus	−50, −2, 30	52, −1, 27
Precuneus	−14, −64, 43	13, −63, 42
Rectal Gyrus	−7, 30, −22	7, 32, −23
Subcallosal Gyrus	−10, 8, −11	11, 8, −11
Sub-Gyral	−35, −23, 0	36, −21, −4
Superior Frontal Gyrus	−17, 38, 31	18, 41, 26
Superior Occipital Gyrus	−36, −82, 28	36, −82, 28
Superior Parietal Lobule	−25, −59, 55	27, −60, 54
Superior Temporal Gyrus	−50, −18, 1	51, −17, 1
Supramarginal Gyrus	−57, −47, 30	58, −48, 30
Transverse Temporal Gyrus	−55, −19, 13	61, −12, 14
Uncus	−27, −6, −28	26, −4, −28

ules: frontal, temporal, parietal and occipital for one hemisphere and the eight different lobules for two hemispheres. The Brodmann areas associated with the 33 anatomical ROIs (left and right hemisphere) are in the left column of Table II.

Table III shows the average Talairach atlas *x*, *y*, *z* coordinates for the 33 left and 33 right hemisphere ROIs. The average coordinates were computed by summing the *x*, *y*, and *z* values of all voxels inside of an ROI and then dividing by the number of voxels.

RESULTS

Mean Absolute Current Density in Low, Middle, and High IQ Groups

In order to evaluate the relationship between LORETA current density and IQ, a low IQ (<90 IQ, n = 80) and high IQ group (>120 IQ, n = 97) comparison as well as an intermediate IQ group analysis (full-scale IQ > 90 < 120, n = 259) was computed using the hypothesis that the cortical current density of the intermediate IQ group will be greater than the low IQ group but less than the high IQ group. The results of the analysis are shown in Figures 1 and 2, which show the average LORETA current density for the low IQ, middle IQ, and high IQ groups in the five different exemplar ROIs. Figure 2 is the same as Figure 1, but only shows the frequency range from 12–30 Hz. Figures 1 and 2 show that the hypothesis was confirmed because all anatomical regions showed an ordered relationship between IQ and LORETA current density, with the lowest current densities associated with the low IQ group, the intermediate LORETA currents associated with the intermediate IQ groups, and the highest current densities associated with the high IQ group. A clear 9 Hz peak difference was present in most of the

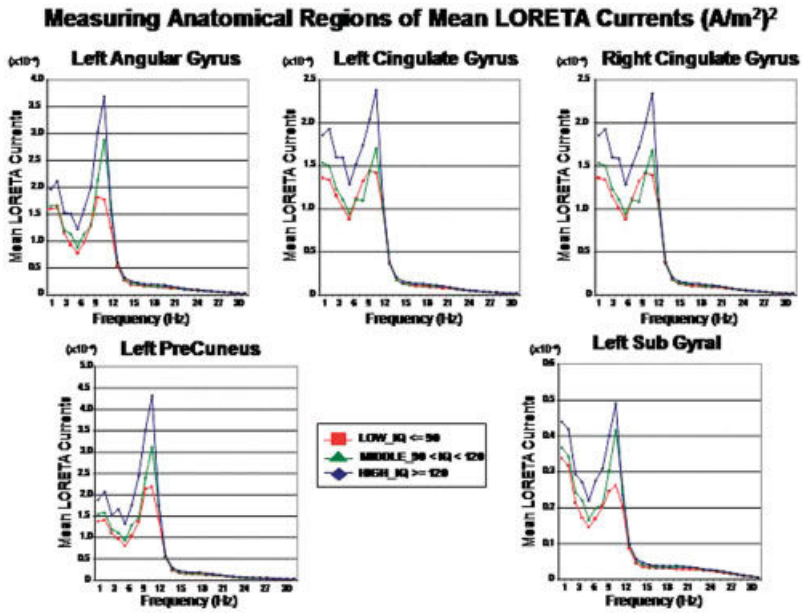

Figure 1.
Mean absolute current densities in exemplar ROIs (angular gyrus, cingulate gyrus, precuneus, and subgyral) for low IQ (≤90 IQ), middle IQ (90 < IQ < 120), and high IQ (≥120 IQ) groups. The *y*-axes are mean LORETA absolute current densities $(A/m^2)^2$ and the *x*-axis is frequency from 1–30 Hz. [Color figure can be viewed in the online issue, which is available at www.interscience.wiley.com.]

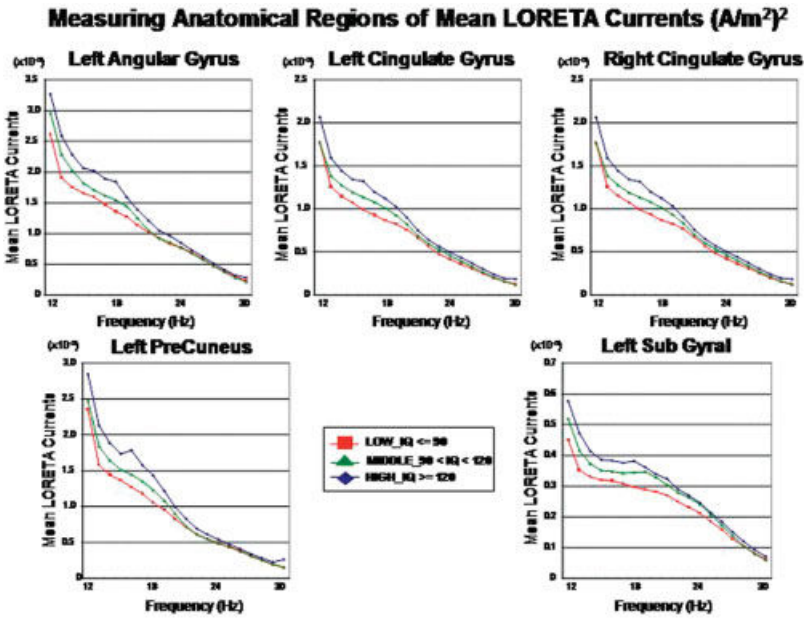

Figure 2.
View of the higher frequency range with mean absolute current densities in exemplar ROIs (angular gyrus, cingulate gyrus, precuneus, and subgyral) for low IQ (≤90 IQ), middle IQ (90 < IQ < 120), and high IQ (≥120 IQ) groups. The *y*-axis are mean LORETA absolute current densities $(A/m^2)^2$ and the *x*-axis is frequency from 12–30 Hz. [Color figure can be viewed in the online issue, which is available at www.interscience.wiley.com.]

ROIs, with frontal regions showing the least difference between high and low IQ, at 9 Hz.

Absolute Current Density of ROIs in High IQ vs. Low IQ Groups

Before computing individual *t* tests, the overall *F* was evaluated in an analysis of covariance (ANCOVA) [Velleman, 1997] with high vs. low IQ groups as the dependent variable, age as a covariate, and frequency and ROIs as the independent variables and Bonferroni correction for multiple comparisons. Table IV shows the *F* values and *P* values for the 33 left hemisphere and 33 right hemisphere ROIs for the high vs. low IQ groups across frequency. Table V shows the *F* values and *P* values for the 30 frequencies for the high vs. low IQ groups across ROIs. These analyses show anatomical and frequency specific differences between high and low IQ groups for different ROIs and different frequencies. The right hemisphere *F* values were higher than the left hemisphere in almost all cases and the frequency range from 22–29 Hz was not statistically significant in the left hemisphere, whereas all frequencies were statistically significant in the right hemisphere. For example, in Table IV it can be seen that the right orbital frontal gyrus had an *F* value of 30.7 ($P < 0.0001$), whereas the homologous left frontal orbital gyrus had an *F* value of 3.02 ($P < 0.08$) in the 22–29 Hz range.

A more detailed analysis is shown in Figure 3, which are the results of *t* tests between the low IQ group (≥70 IQ, ≤90 IQ, n = 80) and the high IQ group (≥120 IQ, n = 97) for the 33 left hemisphere anatomical ROIs. The *y*-axes are *t* values and the *x*-axes are frequencies from 1–30 Hz. The degrees of freedom (df) for each *t* test = 177, which means that for $t = 2.0$, $P < 0.05$; $t = 2.5$, $P < 0.01$; $t = 3.0$, $P < 0.003$; $t = 3.5$, $P < 0.0005$, and $t = 4.0$, $P < 0.000009$. The red horizontal line shows $t = 2.0$, $P < 0.05$. Figure 4 shows the results of *t* tests between the low and high IQ groups for the 33 right hemisphere anatomical ROIs. It can be seen that most of the statistically significant differences were between 1–4 Hz, between 8–9 Hz, between 12–13 Hz, and between 17–18 Hz and 30 Hz with 9 Hz as the most statistically significant frequency band. The least statistically significant differences were in the higher frequency range between ~19 Hz and 26 Hz, although the cingulate gyrus and paracentral lobule were statistically significant at $P < 0.05$ throughout the entire frequency spectrum (1–30 Hz). Peak or maximal T values for groups of ROIs were present at specific frequencies, i.e., 4 Hz, 9 Hz, 13 Hz, 18 Hz, and 30 Hz. Comparison of Figures 3 and 4 shows that the right hemisphere exhibited similar levels of statistical significance but that the right hemisphere generally had higher statistical significance.

Relative or Scaled Current Density of ROIs in High IQ vs. Low IQ Groups

Normalizing or scaling all voxels with respect to 1 or a percentage of the total current density has been suggested by Hernandez et al. [1994] as a necessary renormalization. Therefore, the relative LORETA current density also referred to as "Global Scaling" was computed by summing the absolute current values across all voxels and all frequency and then dividing the absolute current density value in each of the 2,394 voxels by the total current density. The results of *t* tests between the high and low IQ groups using relative current values are shown in Figure 5 for the left hemisphere and in Figure 6 for the right hemisphere. As can be seen in Figures 5 and 6, the statistically significant 9 Hz effect of greater current density in high IQ subjects is still present after global scaling.

TABLE IV. MANOVA *F* values and *P* values for the 33 left hemisphere and 33 right hemisphere ROIs for the high vs. low IQ groups across frequency

	IQ groups high vs. low			
	Left hemisphere		Right hemisphere	
ANATOMICAL REGIONs	*F* ratio	Prob	*F* ratio	Prob
Angular Gyrus	23.165	≤0.0001	22.81	≤0.0001
Anterior Cingulate	2.9054	0.0883	8.726	0.0032
Cingulate Gyrus	16.845	≤0.0001	20.554	≤0.0001
Cuneus	31.13	≤0.0001	34.103	≤0.0001
Extra-Nuclear	14.471	≤0.0001	16.198	≤0.0001
Fusiform Gyrus	40.074	≤0.0001	52.641	≤0.0001
Inferior Frontal Gyrus	6.343	0.0118	12.42	0.0004
Inferior Occipital Gyrus	29.143	≤0.0001	32.742	≤0.0001
Inferior Parietal Lobule	11.645	0.0006	17.467	≤0.0001
Inferior Temporal Gyrus	39.903	≤0.0001	51.727	≤0.0001
Insula	29.948	≤0.0001	29.428	≤0.0001
Lingual Gyrus	29.485	≤0.0001	42.289	≤0.0001
Medial Frontal Gyrus	7.5791	0.0059	9.7825	0.0018
Middle Frontal Gyrus	4.3693	0.0366	7.3452	0.0067
Middle Occipital Gyrus	29.42	≤0.0001	37.064	≤0.0001
Middle Temporal Gyrus	36.991	≤0.0001	51.907	≤0.0001
Orbital Gyrus	3.0208	0.0823	30.7	≤0.0001
Paracentral Lobule	13.051	0.0003	13.565	0.0002
Parahippocampal Gyrus	33.336	≤0.0001	42.706	≤0.0001
Postcentral Gyrus	13.881	0.0002	19.354	≤0.0001
Posterior Cingulate	31.809	’0.0001	38.006	≤0.0001
Precentral Gyrus	9.0254	0.0027	13.004	0.0003
Precuneus	21.383	≤0.0001	23.728	≤0.0001
Rectal Gyrus	6.4678	0.0110	7.4155	0.0065
Subcallosal Gyrus	10.983	0.0009	17.81	≤0.0001
Sub-Gyral	19.542	≤0.0001	52.897	≤0.0001
Superior Frontal Gyrus	7.4278	0.0064	14.648	0.0001
Superior Occipital Gyrus	24.885	≤0.0001	27.822	≤0.0001
Superior Parietal Lobule	12.32	0.0005	11.617	0.0007
Superior Temporal Gyrus	32.305	≤0.0001	45.831	≤0.0001
Supramarginal Gyrus	20.258	≤0.0001	24.278	≤0.0001
Transverse Temporal Gyrus	16.802	≤0.0001	32.527	≤0.0001
Uncus	24.691	≤0.0001	21.274	≤0.0001

However, distortions of the distribution of currents are also present due to the high absolute current density values between 1 and 3 Hz in the frontal ROIs, which can be seen in Figures 1 and 2. For example, unlike the absolute current density *t* tests, relative current density exhibited statistically significant negative *t* values in the delta frequency band (1–4 Hz) in the frontal regions (e.g., anterior cingulate gyrus, orbital gyrus, subcallosal gyrus, and rectal gyrus) and negative *t* values over the 11–28 Hz frequency. The presence of negative Z scores in the delta band and in the higher frequency bands are due to the high levels of current density in the 1–3 Hz band, primarily in the frontal ROIs and not because of reduced current density in the high IQ groups in these frequencies. This conclusion is based on the distribution of absolute current values that are shown in Figures 1 and 2. For example, the high IQ groups exhibited greater absolute current density than the middle IQ and low IQ groups at all frequencies, and there is no evidence of reduced current density in the high IQ groups such as is represented by dividing by the total current density, as in Figures 5 and 6. To evaluate the distortion effect of “global scaling” we recomputed the relative values but omitted the 1–3 Hz frequency band. These analyses, which omitted the low frequency currents, reversed the sign of the *t* tests and resulted in peak differences between the high and low IQ groups more similar to Figures 3 and 4.

Absolute Current Density Differences in High vs. Low IQ Groups in Lobules

In order to evaluate general differences between regions of the brain the ROIs were organized into four left hemisphere and four right hemisphere Brodmann area groups of averaged LORETA current densities. The Brodmann areas that were averaged are shown in Table II. The first column in Table II lists the 33 anatomical ROIs that are sorted by anatomical lobules with corresponding Brodmann areas. The anatomical lobules were: 1, left and right frontal cortical regions; 2, left and right temporal cortical regions; 3, left and right parietal cortical regions; and 4, left and right occipital cortical regions.

TABLE V. MANOVA *F* values and *P* values for the 30 frequencies for the high vs. low IQ groups across ROIs

	IQ groups high vs. low			
	Left hemisphere		Right hemisphere	
	F ratio	Prob	*F* ratio	Prob
FREQ 1	14.652	≤0.0001	35.164	≤0.0001
FREQ 2	31.333	≤0.0001	49.96	≤0.0001
FREQ 3	30.46	≤0.0001	44.687	≤0.0001
FREQ 4	82.925	≤0.0001	123.98	≤0.0001
FREQ 5	55.231	≤0.0001	67.026	≤0.0001
FREQ 6	17.661	≤0.0001	20.542	≤0.0001
FREQ 7	20.578	≤0.0001	29.407	≤0.0001
FREQ 8	41.404	≤0.0001	72.304	≤0.0001
FREQ 9	114.2	≤0.0001	176.53	≤0.0001
FREQ 10	24.728	≤0.0001	40.344	≤0.0001
FREQ 11	5.2641	0.0218	24.444	≤0.0001
FREQ 12	32.993	≤0.0001	91.262	≤0.0001
FREQ 13	68.933	≤0.0001	113.52	≤0.0001
FREQ 14	45.123	≤0.0001	70.288	≤0.0001
FREQ 15	25.955	≤0.0001	41.632	≤0.0001
FREQ 16	45.767	≤0.0001	61.315	≤0.0001
FREQ 17	52.582	≤0.0001	71.396	≤0.0001
FREQ 18	79.648	≤0.0001	94.235	≤0.0001
FREQ 19	50.294	≤0.0001	65.342	≤0.0001
FREQ 20	24.896	≤0.0001	54.934	≤0.0001
FREQ 21	9.5246	0.002	36.91	≤0.0001
FREQ 22	3.3601	0.0668	22.424	≤0.0001
FREQ 23	3.2439	0.0717	24.941	≤0.0001
FREQ 24	0.72437	0.3948	15.828	≤0.0001
FREQ 25	1.3577	0.2440	13.093	0.0003
FREQ 26	0.69371	0.4049	6.5136	0.0107
FREQ 27	2.3902	0.1222	10.268	0.0014
FREQ 28	1.1904	0.2753	6.3978	0.0115
FREQ 29	3.5363	0.0601	10.623	0.0011
FREQ 30	7.0094	0.0028	10.498	0.0012

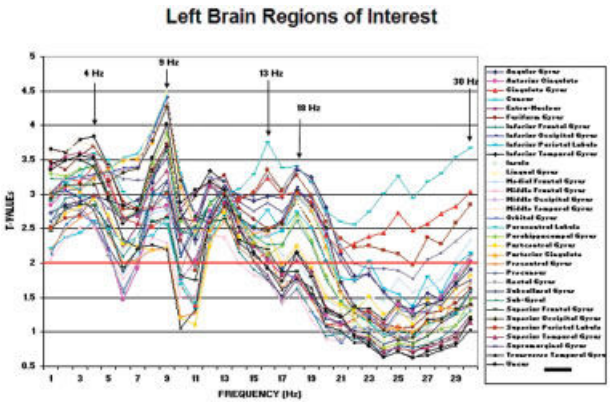

Figure 3.

T values were computed between the absolute source currents in the high IQ group (>120) and the low IQ group (<90) of subjects for 33 anatomical ROIs in the left hemisphere in frequencies from 1–30 Hz. The *t* values are on the *y*-axis and frequency is on the *x*-axis. Arrows show the frequencies of maximal *t* values for groups of ROIs. [Color figure can be viewed in the online issue, which is available at www.interscience.wiley.com.]

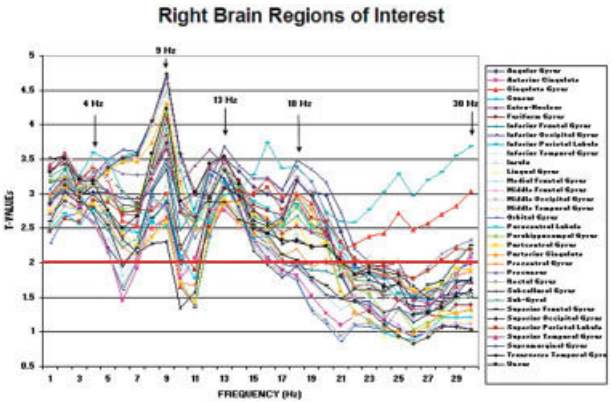

Figure 4.

T values were computed between the absolute source currents in the high IQ group (>120) and the low IQ group (<90) of subjects for 33 anatomical ROIs in the left hemisphere in frequencies from 1–30 Hz. The *t* values are on the *y*-axis and frequency is on the *x*-axis. Arrows show the frequencies of maximal *t* values for groups of ROIs. [Color figure can be viewed in the online issue, which is available at www.interscience.wiley.com.]

Figure 7 shows the *t* test results between the high IQ vs. low IQ groups in the left and right hemisphere lobules. Five different frequencies showed *t* test maxima in different anatomical regions. The *t* test maxima were present at 2–4 Hz, 9–10 Hz, 13–18 Hz, and 29–30 Hz. While all of the anatomical lobules exhibited peaks at these frequencies, the maximal *t* test values were different for different anatomical regions. For example, temporal lobes exhibited maximal *t* test values ($P < 0.0004$) at 4 Hz, the occipital lobes exhibited

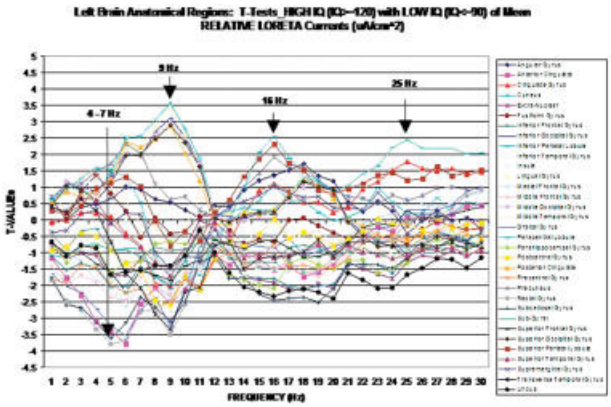

Figure 5.

T values were computed between the relative source currents in the high IQ group (>120) and the low IQ group (<90) of subjects for 33 anatomical ROIs in the left hemisphere in frequencies from 1–30 Hz. The *t* values are on the *y*-axis and frequency is on the *x*-axis. Arrows show the frequencies of maximal *t* values for groups of ROIs. [Color figure can be viewed in the online issue, which is available at www.interscience.wiley.com.]

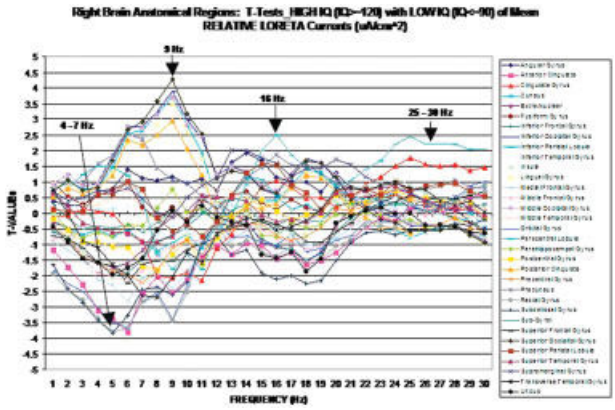

Figure 6.

T values were computed between the relative source currents in the high IQ group (>120) and the low IQ group (<90) of subjects for 33 anatomical ROIs in the left hemisphere in frequencies from 1–30 Hz. The *t* values are on the *y*-axis and frequency is on the *x*-axis. Arrows show the frequencies of maximal *t* values for groups of ROIs. [Color figure can be viewed in the online issue, which is available at www.interscience.wiley.com.]

maximal *t* test values ($P < 0.000009$) at 9 Hz, the temporal lobes exhibited a second maximal *t* test values ($P < 0.0005$) at 13 Hz, the parietal lobes exhibited maximal *t* test values ($P < 0.0007$) at 18 Hz, and the parietal and frontal areas lobes exhibited maximal *t* test values ($P < 0.019$) at 30 Hz. Figure 8 illustrates the anatomical difference in maximal *t* test values at different frequencies in the different Brodmann lobules. Figure 8 shows the average of the left and right *t* values shown in Figure 7. The temporal lobes exhibited maximal *t* value differences between high and low IQ groups at 4 Hz and 13 Hz, the maximal *t* values in the parietal lobes were at 18 Hz, the maximal *t* values in the occipital regions were at 9 Hz and the frontal and parietal lobes exhibited another maxima at 30 Hz. This shows that anatomically differentiated populations of cells exhibit different resonant frequencies of cortical current sources as they correlate to intelligence. All of the averaged Brodmann areas or lobules tended to show increased *t* values between 28–30 Hz; however, only the parietal lobes and frontal lobes were statistically significant ($P < 0.019$) at 30 Hz.

Figure 9 shows the anatomical distribution of maximal *t* values between low and high IQ groups in the Brodmann area lobules at 4 Hz, 9 Hz, 13 Hz, 18 Hz, and 30 Hz. It can be seen that there were different anatomical distributions of maximal *t* values in different Brodmann areas. The left temporal lobes exhibited maximal *t* values at 4 Hz ($t = 3.58$, $P < 0.0004$), the bilateral occipital lobes exhibited maximal *t* values at 9 Hz ($t = 4.57$, $P < 0.000009$), the right temporal lobes exhibited maximal *t* values at 13 Hz ($t = 3.43$, $P < 0.0007$), the bilateral occipital lobes and midline cingulate gyrus exhibited maximal *t* values at 18 Hz ($t = 3.06$, $P < 0.0025$), and the right occipital lobes and midline cingulate gyrus exhibited maximal *t* values at 30 Hz ($t = 2.35$, $P < 0.019$). The global maximum *t* values for all frequencies and all slices were at 9 Hz in the bilateral occipital lobes ($P < 9 \times 10^{-6}$).

Analysis of Covariance with Hemisphere and Current Density as Factors and IQ as the Dependent Variable

ANCOVAs were conducted with high vs. low IQ groups as the dependent variable and current density, Brodmann area lobules and the left and right hemisphere as factors, and age as a covariate [Velleman, 1997]. Although there were no differences in age between IQ groups, the entry of age as a covariate removed possible correlations between the EEG factors and age; thus, the results of the ANCOVA were independent of age. The results of the ANCOVA using Bonferroni corrections for multiple comparisons showed that the four Brodmann area lobules were significantly different between high, middle, and low IQ groups but that there were no significant differences between left and right hemispheres for low vs. high IQ groups. The current density factor was also statistically significant between high, middle, and low IQ groups for all eight Brodmann area lobules (left and right hemisphere) ($F = 135.51$, $P < 0.0001$).

ANCOVA with Bonferroni correction were also conducted using current density as the dependent variable and the factors being the left and right hemisphere, the low, middle, and high IQ groups and four Brodmann area lobules with age again entered as a covariate. The results of the analysis showed a statistically significant difference between left and right hemispheres ($F = 8.89$, $P < 0.0029$) with the right hemisphere having higher mean current density than the left hemisphere for all four anatomical regions. The IQ groups were statistically

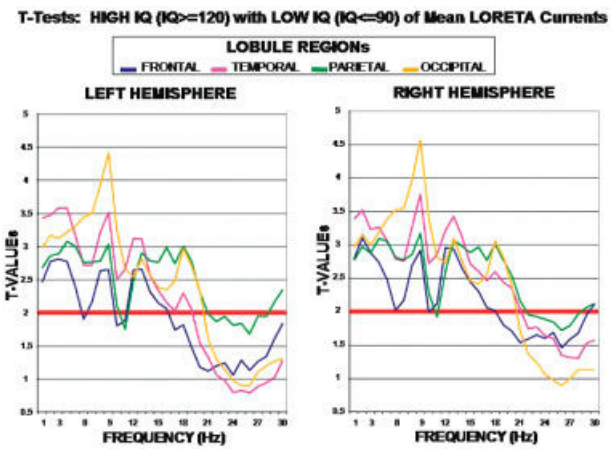

Figure 7.

Left are the *t* test values (*y*-axis) in analyses of the differences in current densities in high vs. low IQ groups from the left hemisphere Brodmann areas in frontal, temporal, parietal, and occipital areas 1–30 Hz (*x*-axis). The right are the *t* test values (*y*-axis) of the differences in current densities in the homologous right hemisphere, 1–30 Hz (*x*-axis). [Color figure can be viewed in the online issue, which is available at www.interscience.wiley.com.]

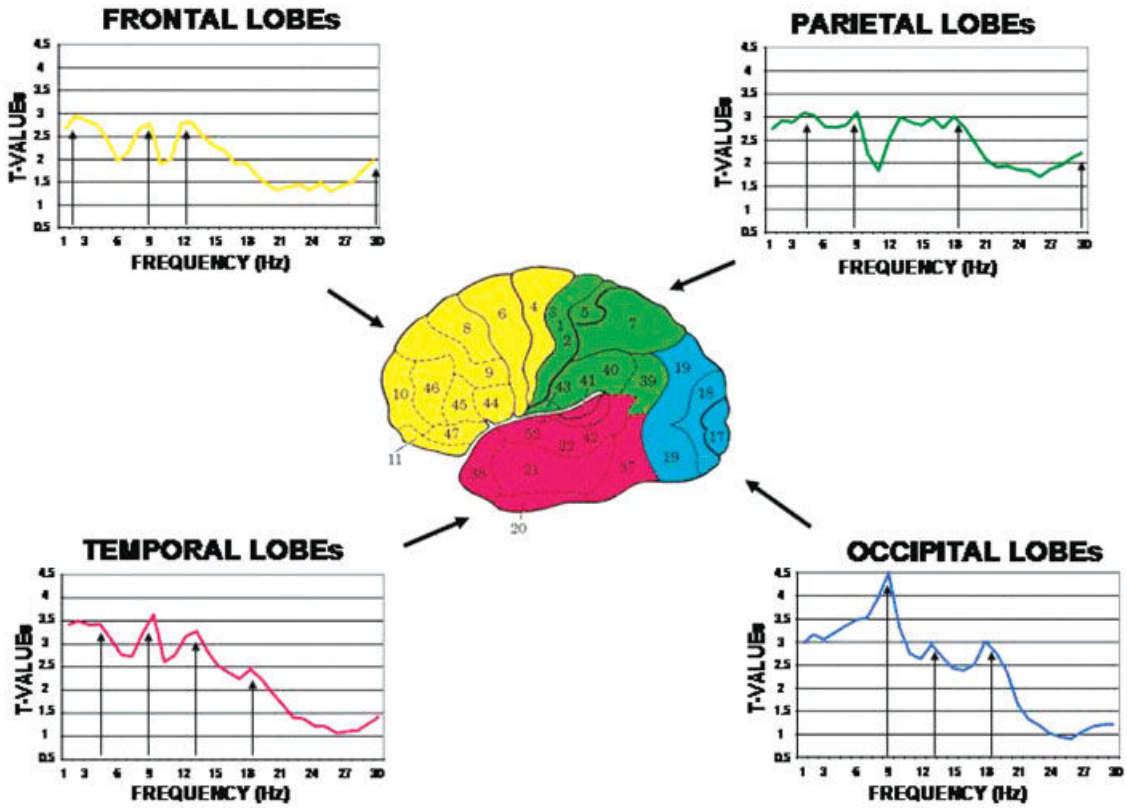

Figure 8.

T values from the average of the left and right hemisphere current densities in high vs. low IQ groups from the frontal, temporal, parietal, and occipital Brodmann lobules as in Figure 3. The center is the Brodmann areas from which the lobules were computed (Table II). The arrows point to the five frequency maxima, 4 Hz, 9 Hz, 13 Hz, 18 Hz, and 30 Hz that have different maxima in different anatomical lobules. This figure shows that while there are shared maxima, nonetheless, different resonant frequencies in low vs. high IQ groups are consistently present in different anatomical regions. [Color figure can be viewed in the online issue, which is available at www.interscience.wiley.com.]

significant ($F = 213.02$, $P < 0.0001$) and the high IQ group with the greatest mean current density for all four Brodmann area lobules. Finally, Brodmann area lobules were statistically significant ($F = 376.51$, $P < 0.0001$) with the parietal lobe effect size of mean current density being the largest.

Linear Relations between Cortical Current Density and IQ

In order to explore the linearity and sensitivity between cortical current density and IQ the subjects were further subdivided into seven full-scale IQ groupings and then linear regression analyses were conducted using cortical currents at 9 Hz as the independent variable and IQ as the dependent variable. The seven IQ groups were: 70–79 IQ (n = 22); 80–89 IQ (n = 49); 90–99 IQ (n = 76); 100–109 IQ (n = 108); 110–119 IQ (n = 83); 120–129 IQ (n = 60); 130–154 IQ (n = 37). The results of the linear regression analyses are shown in Figure 10. Table VI is a rank-ordered list of anatomical regions with statistically significant regression equations. Table VI shows the correlation coefficients for the anatomical ROIs with correlations that range from 0.76 ($P < 0.01$) to a correlation of 0.99 ($P < 0.0001$). It can be seen that statistically significant linear regressions were present in which cortical current density was positively related to full-scale IQ, especially in temporal and parietal regions. Of the 66 anatomical regions 95.45% were statistically significant at $P < 0.05$ and 75.75% were statistically significant at $P < 0.01$ and 31.8% were statistically significant at $P < 0.001$. As seen in Figure 10, the linear regression equation yields an intercept of 25–40 IQ and an approximate average of 7×10^{-4} $(A/m^2)^2$ slope or increment in LORETA current density on the *x*-axis to a 1 IQ point increment on the y-axis. It is important to note that this regression equation is based on only seven points or the averages of seven different groups (n = 442), which means that there are only 6 df and, therefore, this simple linear equation represents a general trend and is not predictive for individual subjects.

DISCUSSION

The findings in this study are consistent with other studies that have shown a positive relationship between the ampli-

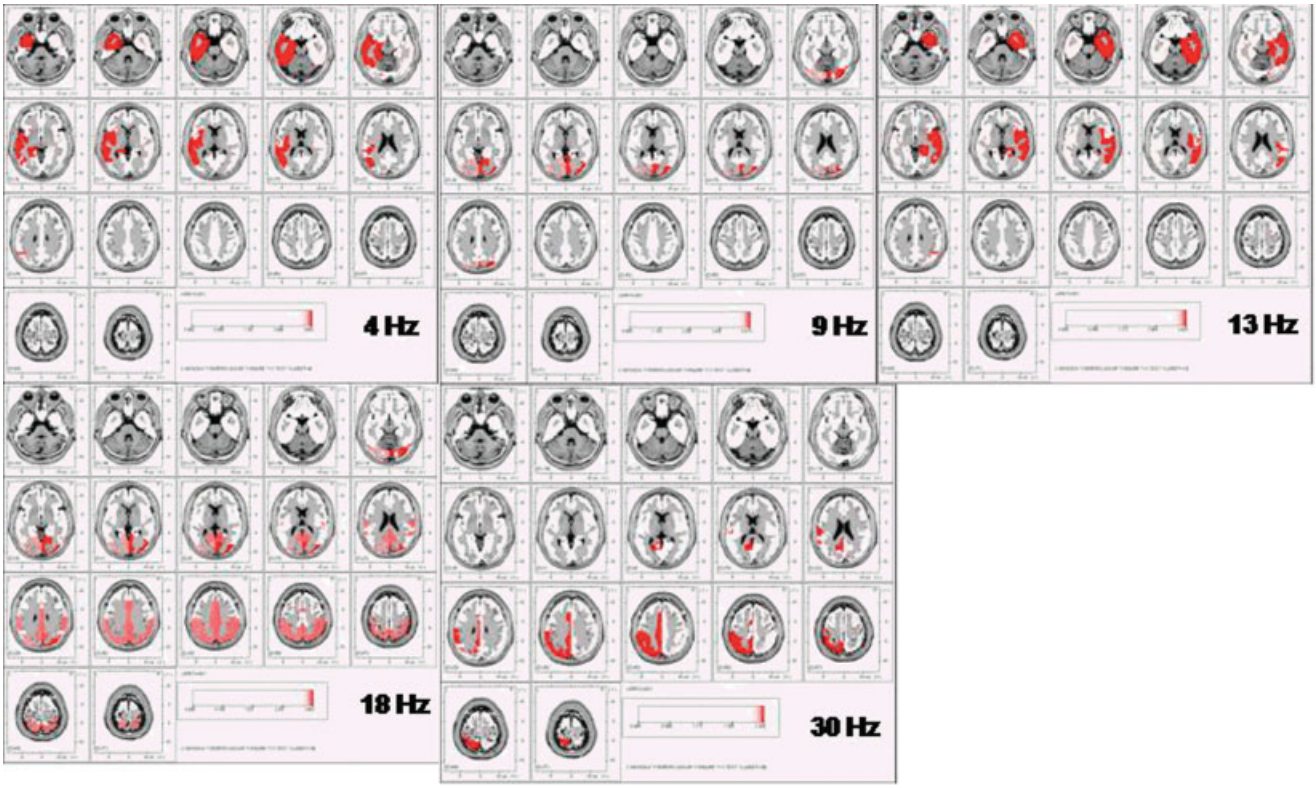

Figure 9.
The anatomical distribution of maximal *t* values between low and high IQ groups in the Brodmann area lobules at 4 Hz ($t = 3.58$, $P < 0.0004$), 9 Hz ($t = 4.57$, $P < 0.000009$), 13 Hz ($t = 3.42$, $P < 0.0007$), 18 Hz (3.06, $P < 0.0025$), and 30 Hz ($t = 2.35$, $P < 0.019$). [Color figure can be viewed in the online issue, which is available at www.interscience.wiley.com.]

tude of the EEG and intelligence; especially in the low to mid alpha frequency range 9–10 Hz [Giannitrapani, 1985; Jausovec and Jausovec, 2001; Marosi et al., 1994; Martin-Loeches et al., 2001; Thatcher et al., 1998, 2001, 2005]. The results are also consistent with the study of Jausovec and Jausovec [2003] that showed a positive relationship between current

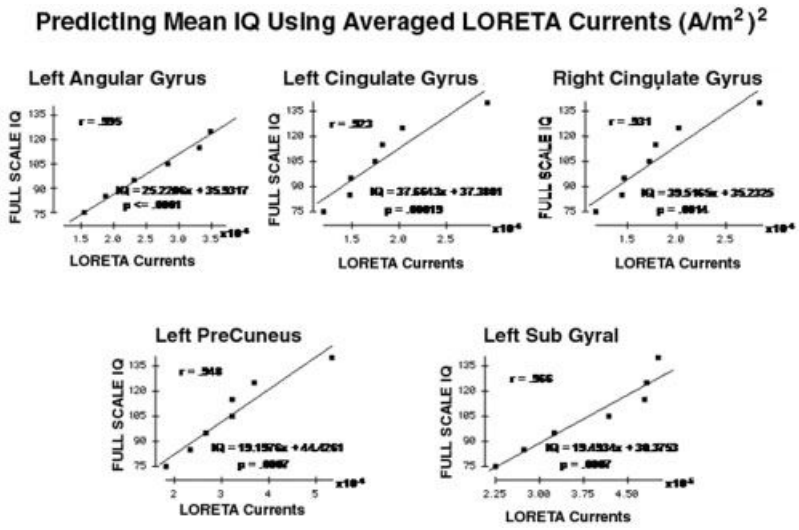

Figure 10.
Linear fit of mean LORETA current density in different anatomical regions for seven IQ groups of subjects: 70–79 IQ (n = 23); 80–89 IQ (n = 49); 90–99 IQ (n = 76); 100–109 IQ (n = 108); 110–119 IQ (n = 83); 120–129 IQ (n = 60); 130–154 IQ (n = 37). The *x*-axis is average current density $(A/m^2)^2$ and the *y*-axis is full-scale IQ.

TABLE VI. Correlation coefficients and intercepts for different regions of interest fit by the linear regression of 7 average IQ groups

Anatomical regions	Intercepts	Coefficients	Correlations
R_Inferior Parietal Lobule	41.89935954	36.06368729	0.768
L_Inferior Frontal Gyrus	58.87194848	227.3750545	0.770
L_Postcentral Gyrus	33.0089669	91.43083127	0.779
R_Middle Occipital Gyrus	46.25947884	22.23929798	0.779
L_Precuneus	46.70457372	18.18158259	0.781
L_Orbital Gyrus	12.29072807	422.7124854	0.784
L_Fusiform Gyrus	36.87745332	66.28303048	0.786
L_Inferior Temporal Gyrus	37.42395311	66.00665266	0.789
R_Precentral Gyrus	47.46416614	148.2036586	0.791
L_Rectal Gyrus	15.54810148	444.4950482	0.794
R_Posterior Cingulate	42.75940252	11.8428397	0.805
R_Orbital Gyrus	11.77536875	401.3824017	0.806
R_Lingual Gyrus	51.15305386	15.27968473	0.812
R_Uncus	48.29278722	156.3282876	0.812
R_Anterior Cingulate	28.84632612	223.5249793	0.817
R_Rectal Gyrus	15.60483641	458.6398408	0.835
L_Uncus	45.0802762	213.0697025	0.842
L_Anterior Cingulate	29.28880334	217.4746016	0.852
R_Superior Temporal Gyrus	34.96590934	44.29983711	0.855
R_Middle Frontal Gyrus	58.61840255	146.5004948	0.861
R_Postcentral Gyrus	28.57800568	88.29575325	0.862
L_Superior Frontal Gyrus	36.32603286	210.8986535	0.863
R_Inferior Frontal Gyrus	67.18196885	110.1715478	0.866
R_Fusiform Gyrus	45.64514447	43.57660614	0.885
R_Precuneus	42.77310497	18.08633556	0.890
R_Transverse Temporal Gyrus	11.88012311	117.4105799	0.901
L_Transverse Temporal Gyrus	11.93193643	105.9073691	0.911
R_Superior Frontal Gyrus	45.82393401	203.8939981	0.914
L_Insula	25.10576493	300.2323413	0.920
R_Inferior Temporal Gyrus	43.79259455	47.57089306	0.926
L_Supramarginal Gyrus	32.41819968	52.88458516	0.937
R_Subcallosal Gyrus	22.59695616	616.3256466	0.946
L_Subcallosal Gyrus	17.8759402	804.5373848	0.952
R_Insula	40.57402443	110.5541468	0.965
L_Middle Temporal Gyrus	36.23732315	36.29340468	0.970
R_Middle Temporal Gyrus	38.35589548	30.97856726	0.973
R_Sub-Gyral	44.35339181	140.7011771	0.978
R_Supramarginal Gyrus	43.30628227	18.0416313	0.982
L_Sub-Gyral	32.02469417	188.1692283	0.988
L_Angular Gyrus	37.83671457	24.18321448	0.995
Mean at $P < 0.001$	34.53981512	197.5393517	0.960980533
Mean at $P < 0.05$	36.18379819	167.5011766	0.868519854

density and IQ using LORETA although only relative currents (50% above maximum) were reported. Jausovec and Jausovec [2003] found a relationship between the FWHM or the spatial spread of currents to be less in high IQ subjects than in lower IQ subjects, which is consistent with a steeper and more spatially focused current in high IQ subjects. In the present study the maximum difference in current density between high and low IQ groups was at 9 Hz (see Figs. 1–4) which exhibited a smaller spatial spread than at other frequencies, i.e., a smaller FWHM. There were no statistically significant differences in mean age between the different IQ groups and ANCOVA with age as the covariate adjusted for a possible age effect. Therefore, age differences cannot account for the findings in this study.

Importantly, frequency analyses of the surface EEG showing higher amplitudes between the same high and low IQ subjects in the Thatcher et al. [2005] study are consistent with the LORETA current density findings in the present study. For example, the strength of the surface EEG alpha, delta, and beta band correlations in Thatcher et al. [2005] were also present with LORETA 3D current densities at the same frequency bands and corresponding locations, i.e., alpha in posterior regions, etc.

This study was not an active task design; instead, alert but resting EEG was recorded and the intelligence tests were administered on the same day but at a different time. The difference between active task designs and resting EEG designs are important when comparing different studies. The relationship between current density and intelligence showed a medium to strong effect size in a large number of voxels, especially at 9 Hz (see Figs. 1–6) and especially in parietal and occipital regions using either absolute or relative current density.

Limitations of This Study

Although systematic differences in current density were observed between high, medium, and low IQ subjects; nonetheless, there are limitations of this study which are important when considering future studies on this subject. One limitation is the low sample rate (128 Hz) and reduced frequency range from 1–30 Hz since the gamma frequency range has been shown to be important in several EEG studies of cognition [Jensen and Lisman, 1998; John, 2002]. In addition, due to space limitations correlations between current density and WISC-R subtests or verbal vs. performance IQ were not analyzed. The use of a linked ears reference does not appear to be a limitation because average reference analyses yielded nearly identical results. Because of space limitations the results of the average reference analyses were not included in this study. Finally, this study focused primarily on the age range of 5–20 years and only a small number of adult and older subjects were included. More detailed developmental analyses, especially of the elderly during periods of cognitive decline may provide additional insight into the relationship between intelligence and current density.

Cortical Current Density and Intelligence

The findings of this study are that, in general, the higher the cortical current density at specific frequencies and locations, the higher the IQ. While there were specific anatomical locations and right hemisphere dominance as well as some frequencies that exhibited maximal *t* values; nonetheless, there was generally a greater mean source current present in high IQ subjects compared to low IQ subjects. A global scale factor such as by Hernandez et al. [1994] cannot account for the results because of frequency and anatomical specificity and because there were no significant differences in age between the low, middle, and high IQ groups and the subjects were recruited randomly without knowledge of their subsequent IQ performance or skull thickness or skin resistance and skull size. Further, the use of a global scale factor or relative current density such as in Figures 5 and 6 emphasized the strength of the 9 Hz effect but also distorted the effects due to the high absolute current density values in the frontal ROIs between 1–3 Hz. The problem with relative current values is that high current values in a given frequency or ROI distorts the distribution, which means that one must evaluate the absolute current values in order to interpret the relative values. For example, the relative or global scaling resulted in negative *t* test values in the theta frequency band and in higher frequency bands (see Figs. 5, 6), thus indicating that there is less current density in high IQ subjects compared to low IQ subjects. However, examination of the absolute current density values in Figures 1 and 2 show that there are no instances in which there is less current density in high IQ subjects compared to middle or low IQ subjects, and therefore the findings in Figures 5 and 6 represent a distortion due to the process of summing all currents at all frequencies and then dividing each voxel with respect to the total. The weakness of a relative or global normalization is its dependence on inspection of the absolute values in order to interpret the relative measure. For example, artifact in one region or a spike discharge in one region can distort the percentage in all regions if a relative measure is used. Absolute measures allow one to subtract the effects of an artifact or a spike or rhythmic processes, whereas relative measures do not allow for this. We conclude that the use of a global scaling factor such as by Hernandez et al. [1994] should be conducted with caution and not be used without evaluation of the absolute values in order to interpret the scaled values.

The absolute and relative measures were consistent by showing significant differences at specific frequencies and locations, although with different signs, both methods demonstrate a widespread and wide band differences between high and low IQ groups. A finding of a wide frequency range using absolute and/or relative current sources over a wide anatomical distribution, which cannot be accounted for by skull conductivity indicates a brainstem and/or diffuse thalamic modulating effect on general cortical excitability. For example, the reticular formation exerts a broad frequency range of modulatory control over the excitatory drives influencing widespread cortical pyramidal cells [Lindsley, 1961; Scheibel and Scheibel, 1958]. In contrast, a frequency-specific effect such as the finding of a dominant 2–4 Hz, 9–10 Hz, 13–18 Hz, and 20–30 Hz difference between high and low IQ groups in absolute current density is consistent with a resonance process that is likely of a thalamo-cortical and/or cortico-cortical origin [Llinas and Ribary, 1998; Nunez, 1981, 1994; Lehar, 2000].

Local Generator Synchrony and Current Density

The amplitude of the EEG is not a simple matter of the total number of active neurons and synapses. The importance of the synchrony of a small percentage of the synaptic sources of EEG generators is far greater than the total number of generators. For example, Nunez [1981, 1994] and Lopes da Silva [1994] have shown that the total population of synaptic generators of the EEG are the summation of: 1, a synchronous generator (M) compartment, and 2, an asynchronous generator (N) compartment in which the relative contribution to the amplitude of the EEG = $M\sqrt{N}$. This means that synchronous generators contribute much more to the amplitude of EEG than asynchronous generators. For example, assume 10^5 total generators in which 10% of the generators are synchronous or $M = 1 \times 10^4$ and $n = 9 \times 10^4$ then EEG amplitude = , or in other words, a 10% change in the number of synchronous generators results in a 33-fold increase in EEG amplitude [Lopez da Silva, 1994]. Blood flow studies of intelligence often report fewer blood flow changes in high IQ groups compared to lower IQ subjects [Haier et al., 1992; Haier and Benbow, 1995; Jausovec and Jausovec, 2003]. Cerebral blood flow is generally related to the total number of active neurons integrated over time, e.g., 10–20 min [Herscovitch, 1994; Yarowsky et al., 1983, 1985]. In contrast, EEG amplitude as described above is influenced

by the number of synchronous generators much more than by the total number of generators and this may be why high IQ subjects while generating more synchronous source current than low IQ subjects often fail to show greater cerebral blood flow. As mentioned previously, this conclusion is consistent with the LORETA studies by Jausovec and Jausovec [2003] that showed a steeper FWHM in high IQ subjects, which is expected when there is focal or localized synchronization.

Linear Regression of Current Density and Intelligence: A "Ground State" of Cognition

To give perspective, the effect size or magnitude of correlation between IQ and current density was low for individual voxels, on the order of 0.15–0.25 at n = 442. Further, the individual and combined effect size of current density was less than the effect size for EEG phase and EEG coherence observed in Thatcher et al. [2005]. The relative ranking of effect size remains, EEG phase > EEG coherence > EEG amplitude asymmetry > power including current density. Average IQ measures were used to compute the linear regression fits in Figure 10 using averaged ROI pixel groupings and there were significant linear relationships between cortical current density and IQ in many anatomical regions. The purpose of averaging IQ by groupings of 10 IQ points was to evaluate the relative sensitivity of the relationship between IQ and LORETA current density. The rather high correlation values in Table VI are an artifact due to the averaging of a small number of IQ groups (i.e., seven groups, df = 6). Lower correlations are present when using regression based on individual subjects and the group average regression cannot be used to predict individual values. The highest correlations between IQ and current density were in the temporal and parietal lobes with correlations that ranged from 0.92–0.99. Evaluation of the regression equations showed that the intercept when current density = 0 predicted very low IQ scores in the range of 20–45 IQ points. This finding is what is expected if current density was a valid predictor of IQ, that is, the findings are validated because the prediction of IQ when currents = 0 is in the range of intelligence in severely retarded and profoundly retarded individuals. Cortical current density is measured by LORETA because only the cortical pyramidal cells are capable of producing dipoles and, through synchrony, forming equivalent dipole current sources [Nunez, 1981; Scherg, 1990]. Anencephalic humans are born without a neocortex or thalamus yet they exhibit a number of complex, integrative behaviors such as rooting, suckling, crying, smiling, laughing, and pleasurable excitement [Gamper, 1926; Livingston, 1967].

The importance of a linear regression between intelligence and cortical current density is that it predicts an absolute current density "ground state" or "reference estimate," below which there is near zero or minimal current density and above which there is increasing levels of intellectual functioning. The concept of a "ground state" of intelligence may be of value in the development of general theories and models of intelligence based on mechanisms of neural synchrony and resource allocation and may have clinical relevance, for example, in the evaluation of persistent vegetative states [Coleman et al., 2005; Chen et al., 1996].

Anatomical Differences in Cortical Current Density and Intelligence

In general there was slightly greater current density in right hemisphere gray matter voxels than in left hemisphere voxels for all three groups of IQ subjects at all frequencies (Figs. 1, 2). There were marked differences in effect size as a function of anterior vs. posterior cortical regions, with the smallest differences between IQ groups in frontal regions and the strongest differences in posterior and temporal regions. In the Thatcher et al. [2005] study posterior EEG power and frontal amplitude independent measures such as coherence and phase delays were strongly related to IQ The finding of greater cortical currents in occipital cortical regions at 9 Hz in all IQ groups further supports the conclusion that intelligence is related to thalamo-cortical resonance [Nunez, 1981, 1994].

The finding of 9 Hz maximal correlations with IQ is consistent with the findings of Schmid et al. [2002]. Studies by Jausovec and Jausovec [2000a,b] showed that increased power in the high alpha frequency band (10–12 Hz) was more significantly correlated to IQ than increased power in the lower alpha frequency band (e.g., 8–9 Hz). However, genetic studies of the correlation between increased alpha power and increased alpha frequencies have failed to find a correlation between increased alpha frequency and IQ [Posthuma et al., 2001] and other studies have also failed to find a correlation between IQ and the high alpha band [Giannitripani, 1985]. These discrepancies may be irrelevant considering that other frequencies in addition to the alpha frequency range also correlate to intelligence [Giannitripani, 1985; Marosi et al., 1999; Thatcher et al., 2005].

An important finding was the presence of maximal *t* values at different frequencies and in different Brodmann areas of the cortex. This showed that anatomically differentiated populations of cells exhibit different resonant frequencies of cortical current sources in correlation to intelligence. Not all frequencies were significantly related to intelligence; for example, the theta frequencies (5–7 Hz) in absolute current density were generally not statistically significant. An interesting finding was the relationship between the currents from the frontal lobes and the parietal lobes at 30 Hz. Many of the averaged Brodmann areas tended to show increased *t* values between 28–30 Hz; however, only the parietal lobes and frontal lobes were statistically significant at 30 Hz. This finding indicates that only particular ROIs are significant near 30 Hz, which is consistent with the studies of Llinas and Ribary [1998] and John [2002], which show that higher frequency coherence and zero phase lags are often related to cognitive functioning and to levels of consciousness.

Frequency Resonance of Cortical Current Density and Intelligence

As mentioned previously, the finding of a relationship between frequency peaks in certain frequency ranges (e.g., 4 Hz, 9 Hz, 13 Hz, 18 Hz, and 30 Hz) and intelligence is strong evidence of thalamo-cortical and cortico-cortical resonance (i.e., oscillations) as being directly related to intelligence. The importance of neural oscillations and EEG resonance in perception and cognition is well established as being a fundamental property of thalamic and cortical dynamics [Lehar, 2000; Llinas and Ribary, 1998; Purpura, 1959, 1972; Steriade et al., 1991, 1993; Thatcher and John, 1977]. Thalamic cortical input is necessary to maintain EEG resonances, especially at 9–10 Hz [Purpura, 1959, 1972; Steriade et al., 1991, 1993]. It is well established that thalamo-cortical resonance is essential for synchronizing spatially localized cortical neurons as well as spatially distant cortical populations [Llinas and Ribary, 1998; Purpura, 1972; Thatcher and Purpura, 1973] and that cortico-cortical resonances are also major contributors to spatially distributed neural synchrony [Nunez, 1981, 1994].

Synchrony and phase delays are fundamental to the concept of "resonance" in the EEG spectrum, and the thalamus is located near to the center of the brain and thalamic axons extend radially from the thalamus up to a layered sheet of pyramidal cell dendrites that when synchronous produce the human electroencephalogram or EEG [Nunez, 1981, 1994]. One advantage of a centrally located synchronizing structure like the thalamus is the ability to act like a "pacemaker" or the "drummer" and produce near zero phase delays or "phase reset" in widely separated cortical regions by virtue of its central location. To the extent that there is a shift toward an increased number of synchronous generators at a given moment of time, then it is reasonable to conclude that there is a greater signal-to-noise ratio related to an evoking stimulus or to an internally generated activation by intrinsic thalamic pacemaker activity in the spontaneous EEG when no evoking stimulus is present [Purpura, 1959; Steriade et al., 1991; 1993; Thatcher and John, 1977].

Moving Window Model of Intelligence

Although subjective time is experienced as continuous, in fact there is regular thalamic bursting activity that is discontinuous and involved in successive "perceptual frames" that define a "traveling moment of perception" [Allport, 1968; John, 2002; Lehmann et al; 1998; Thatcher and John, 1977; Thatcher, 1997; Varela et al., 1981]. Early studies of perceptual frames demonstrated that sequential stimuli that occur within a "perceptual frame" will be perceived as simultaneous, while events separated by a longer time interval are perceived as sequential [Efron, 1970]. The duration of the perceptual frame, sometimes referred to as an "integration interval" varies depending on the complexity of the stimuli and the modality, but ranges from about 40–250 msec [Efron, 1970].

The brain is not a heart with a few coupled "pacemakers"; instead, the brain has a centrally located "percussion section" called the thalamus that contains a wide spectrum of bursts of excitation arising rhythmically onto the cortex of the human brain, thus significantly influencing the synchrony of generators and the current density of the EEG at each moment of time [Nunez, 1981, 1994]. To develop a model to explain the findings of this study, let us consider that the neurophysiological mechanisms that produce the "perceptual frame" are also operational in the frequency and anatomical localization findings observed in this study. These assumptions are reasonable because the number one candidate for the initiation and distribution of cortical rhythms is the thalamus [John, 2002; Steriade et al., 1991, 1993] and the number one candidate for the production of the EEG is the human neocortex, which is also the number one candidate responsible for intelligence [Nunez, 1981, 1994]. Next, let us hypothesize that:

(1) "Microstates" of increased synchrony of synaptic generators resonate at a particular frequency range over time and the amount of synchrony in a given microstate is directly related to intelligence.
(2) The "microstates" of resonant synchrony of synaptic generators correspond to the frequency maxima that were directly related to IQ in the present study (e.g., Figs. 1–4). To test this hypothesis, let us transform frequency to time by measuring the wavelengths of the approximate centers of the frequency maxima in Figure 8, e.g., 30 Hz = 33 msec; 18 Hz = 55.5 msec; 13 Hz = 77 msec; 9 Hz = 111 msec; and 4 Hz = 250 msec.

According to this model, each moving window or moment of time is composed of a mixture of microstates that are triggered and time locked to the onset of a moving window like a perceptual frame. Figure 11 illustrates the hypothesized moving window model of intelligence. According to this hypothesis the greater the synchrony of functionally localized neural generators within each microstate, then the higher the signal-to-noise ratio within a moving window of intelligence.

In other words, it is hypothesized that higher IQ subjects have greater neural synchrony and greater information processing within a moving window of time mediated by a sequence of thalamo-cortical synchronizing mechanisms. Studies by John [2002], Koenig et al. [2001], Bressler and Kelso [2001], and von Stein and Sarntheim [2000] support the hypothesis that there are a constellation of different frame durations which involve near zero phase lag synchrony across anatomically distributed systems. It is reasonable to postulate that similar near zero phase lag processes are also involved in intelligence. The microstate model is consistent with a thalamo-cortical phase reset process that synchronizes oscillators within local domains of cells and across long-distance networks as described by Freeman [2004]. Finally, it is not clear if the "microstates" measured by Lehmann [1971] and Lehmann et al. [1998] are similar or related to the proposed microstates in this model of intelligence. Future research may clarify this issue.

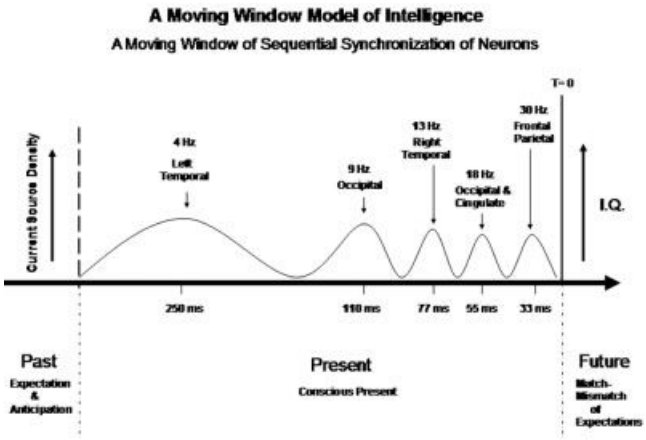

Figure 11.

Moving window model of intelligence. Horizontal arrow is the time flow of the specious present represented by a sequence of "microstates" of synchronous synaptic activity that generated the current density maxima at different frequencies observed in this study (Figs. 1–4). Vertical arrow (left) is current density and increasing signal-to-noise ratio of the microstates and vertical arrow (right) is IQ. The anatomical labels refer to the Brodmann area lobules in Figure 4 and the microstates are current density peaks at 4 Hz (250 msec), 9 Hz (111 msec), 13 Hz (77 msec), 18 Hz (55.5 msec), and 30 Hz (33.3 msec). The conversion from the frequency domain to the time domain of maximal current sources represent synchronously induced resonances by multiple but synchronized thalamo-cortical pacemakers and constitute successive "frames" that define a "traveling moment" [Allport, 1968; Efron, 1970]. The results of this study indicate that the greater the proportion of synchronous generators in a microstate during awake and alert states, then the greater the signal-to-noise ratio of that microstate, which is directly related to intelligence.

Neural Efficiency Model of Intelligence

As mentioned previously, the findings in this study support neural efficiency models of intelligence [Anokhin et al., 1999; Jausovec and Jausovec, 2003; Thatcher et al., 2005]. The combined EEG coherence and phase findings of the previous Thatcher et al. [2005] study and the present findings support a model of efficient allocation of neural resource that is dependent on four factors: 1) Optimal levels of general arousal mediated by brain stem and midline thalamic systems; 2) increased synchronization of localized neural generators constituting distributed microstates within a moving window of time; 3) near zero phase lag synchronization of posterior cortical neurons by the frontal lobes; and 4) high global differentiation or complexity of the brain. Long-distance network synchronization of LORETA currents was not analyzed in this study; however, previous studies of the coherence of the surface EEG found reduced coherence to be related to higher IQ [Thatcher et al., 2005]. This would be expected in a differentiated system of locally synchronized generators if long-distance coordination of cortical synchrony is mediated by a centrally located structure such as the thalamus. The results of the present study and the previous coherence and phase study [Thatcher et al., 2005] support the hypothesis that the ability to synchronize neural generators corresponds to increased efficiency of resource allocation in higher IQ subjects.

ACKNOWLEDGMENTS

We thank Dr. Rebecca McAlaster, Mr. Lang Andersen, and Ms. Sheila Ignasias for administering and scoring the neuropsychological and school achievement tests. We also thank Drs. David Cantor and Michael Lester for involvement in the recruitment, EEG testing, and evaluation of subjects, and Rebecca Walker and Richard Curtin for database management. Informed consent was obtained from all subjects in this study.

REFERENCES

Allport DA (1968): Phenomenal simultaneity and perceptual moment hypotheses. Br J Psychology 59:395–406.

Anokhin AP, Lutzenberger W, Birbaumer N (1999): Spatiotemporal organization of brain dynamics and intelligence: an EEG study in adolescents. Int J Psychophysiol 33:259–273.

Bressler SL, Kelso JA (2001): Cortical coordination dynamics and cognition. Trends Cogn Neurosci 5:26–36.

Chen R, Bolton CF, Young B (1996): Prediction of outcome in patients with anoxic coma: a clinical and electrophysiologic study. Crit Care Med 24:672–678.

Coleman MR, Menon DK, Fryer TD, Pickard JD (2005): Neurometabolic coupling in the vegetative and minimally conscious states: preliminary findings. J Neurol Neurosurg Psychiatry 76:432–440.

Efron E (1970): The relationship between the duration of a stimulus and the duration of a perception. Neuropsychologia 8:37–55.

Freeman W (2004): Origin, structure and role of background EEG activity. Part 1. Analytic amplitude. Clin Neurophysiol 115:2077–2088.

Frei E, Gamma A, Pascual-Marqui RD, Lrhmsnn D, Hell D, Vollenweider FX (2001): Localization of MDMA-induced brain activity in healthy volunteers using low resolution electromagnetic tomography (LORETA). Hum Brain Mapp 14:152–165.

Gamper E (1926): Structure and functional capacity of human mesencephalic monster (arhinen-cephalic with encephalocele); contributions to teratology and fiber systems. Z Ges Neurol Psychiatrie 102:154–235; discussed by Livingston [1967].

Gasser T, Von Lucadpi-Muller I, Verleger R, Bacher P (1983): Correlating EEG and IQ: a new look at an old problem using computerized EEG parameters. Electroencephalogr Clin Neurophysiol 55:493–504.

Giannitrapani D (1985): The Electrophysiology of Intellectual Functions. New York: Kargere Press.

Gomez JF, Thatcher RW (2001): Frequency domain equivalence between potentials and currents using LORETA. Int J Neurosci 107:161–171.

Haier RJ, Benbow CP (1995): Sex difference and lateralization in temporal lobe glucose metabolism during mathematical reasoning. Dev Neuropsychol 4:405–414.

Haier RJ, Siegel B, Tang C, Abes I, Buchsbaum MS (1992): Intelligence and changes in regional cerebral glucose metabolic rate following learning. Intelligence 16:415–426.

Hernandez JL, Valdez P, Biscay R, Virues T, Szava S, Bosch J, Riquenes A, Clark I (1994): A global scale factor in brain topography. Int J Neurosci 76:267–278.

Herscovitch P (1994): Radiotracer techniques for functional neuroimaging with positron emission tomography. In: Thatcher RW, Hallett M, Zeffiro T, John ER, Huerta M, editors. Functional Neuroimaging: Technical Foundations. San Diego: Academic Press.

Jausovec N, Jausovec K (2000a): Differences in resting EEG related to ability. Brain Topogr 12:29–240.

Jausovec N, Jausovec K (2000b): Correlations between ERP parameters and intelligence: a reconsideration. Biol Psychol 55:137–154.

Jausovec N, Jausovec K (2001): Differences in EEG current density related to intelligence. Brain Res Cogn Brain Res 12:55–60.

Jausovec N, Jausovec K (2003): Spatiotemporal brain activity related to intelligence: a low resolution brain electromagnetic tomography study. Brain Res Cogn Brain Res 16:267–272.

Jausovec N, Jausovec K (2004): Differences in induced brain activity during the performance of learning and working-memory tasks related to intelligence. Brain Cogn 54:65–74.

Jensen O, Lisman JE (1998): An oscillatory short-term memory buffer model can account for data on the Sternberg task. J Neurosci 18:10688–10699.

John ER (2002): The neurophysics of consciousness. Brain Res Rev 39:1–28.

Kaiser DA, Sterman MB (2001): Automatic artifact detection, overlapping windows and state transitions. J Neurother 4:85–92.

Koenig T (2001): Topographic time-frequency decomposition of the EEG. Neuroimage 14:383–390.

Lindsley DB (1961): The reticular activating system and perceptual integration. In: Sheer DE, editor. Electrical Stimulation of the Brain. Austin: University of Texas Press. p 331–349.

Livingston RB (1967): Brain circuitry relating to complex behavior. In: Quarton GC, Melenechuk T, Schmidt FO, editors. The Neurosciences: A Study Program. New York: Rockefeller University Press. p 499–515.

Llinas R, Ribary U (1998): Temporal conjunction in thalamocortical transactions. Consciousness: at the frontiers of neuroscience. In: Advances in Neurology, vol. 77. Philadelphia: Lippincott-Raven. p 95–103.

Lopes Da Silva FH (1995): Dynamic of electrical activity of the brain, networks, and modulating systems. In: Nunez P, editor. Neocortical Dynamics and Human EEG Rhythms. New York: Oxford University Press. p 249–271.

Marosi E, Rodriguez H, Harmony T, Yanez G, Rodriquez M, Bernal J, Fernandez T, Silva J, Reyes A, Guerrero V (1999): Broad band spectral parameters correlated with different IQ measurements. Int J Neurosci 97:17–27.

Martin-Loeches M, Munoz-Ruata J, Martinez-Lebrusant L, Gomez-Jari G (2001): Electrophysiology and intelligence: the electrophysiology of intellectual functions in intellectual disability. J Intellect Disabil Res 45:63–75.

Mazziota JC, Toga AW, Evans AC, Fox PT, Lancaster JL (1995): Digital brain atlases. Trends Neurosci 18:210–211.

Nunez P (1981): Electrical Fields of the Brain. New York: Oxford University Press.

Nunez P (1994): Neocortical Dynamics and Human EEG Rhythms. New York: Oxford University Press.

Pascual-Marqui RD (1999): Review of methods for solving the EEG inverse problem. Int J Bioelectromagn 1:75–86.

Pascual-Marqui RD (2003): Free software and documentation from the Key Institute. http://www.unizh.ch/keyinst/NewLORETA/Software/Software.htm.

Purpura DP (1959): Nature of electrocortical potentials and synaptic organizations in cerebral and cerebellar cortex. In: Pfeiffer CC, Smythes JR, editors. International Review of Neurobiology. New York: Academic Press.

Purpura DP (1972): Functional studies of thalamic internuclear interactions. Brain Behav 6:203–234.

Scheibel ME, Scheibel AB (1958): Structural substrates for integrative patterns in the brain stem reticular core. In: Jasper HH, Proctor LD, Knighton RS, Noshay WS, Costello RT, editors. The Reticular Formation of the Brain. Boston: Little Brown. p 31–55.

Scherg M (1990): Fundamentals of dipole source potential analysis. In: Hoke GF, Romani GL, editors. Auditory Evoked Magnetic Fields and Electric Potentials, vol. 6. Advances in audiology. Basel: Karger. p 40–69.

Schmid RG, Tirsch WS, Scherb H (2002): Correlation between spectral EEG parameters and intelligence test variables in school-age children. Clin Neurophysiol 113:1647–1656.

Steriade M, Curró Dossi R, Paré D, Oakson G (1991): Fast oscillations (20-40 Hz) in thalamocortical systems and their potentiation by mesopontine cholinergic nuclei in the cat. Proc Natl Acad Sci U S A 88:4396–4400.

Steriade M, Curró Dossi R, Pare D (1993): Electrophysiological properties of intralaminar thalamocortical cells discharging rhythmic (~40 Hz) spike-bursts at ~1000 Hz during waking and rapid-eye-movement sleep. Neuroscience 56:1–19.

Talairach J, Tournoux P (1988): Co-planar Stereotaxic Atlas of the Human Brain. New York: Thieme Medical.

Thatcher RW (1997): Neural coherence and the content of consciousness. Conscious Cogn 6:42–49.

Thatcher RW, John ER (1977): Functional Neuroscience: Foundations of Cognitive Processing. Mahway, NJ: Lawrence Erlbaum. p 53–111.

Thatcher RW, Purpura DP (1973): Postnatal development of thalamic synaptic events underlying evoked recruiting responses and electrocortical activation. Brain Res 60:2l–24.

Thatcher RW, Biver C, Camacho M, McAlaster R, Salazar AM (1998): Biophysical linkage between MRI and EEG amplitude in traumatic brain injury. Neuroimage 7:352–367.

Thatcher RW, Biver CL, Gomez-Molina JF, North D, Curtin R, Walker RW, Salazar A (2001): Estimation of the EEG power spectrum by MRI T2 relaxation time in traumatic brain injury. Clin Neurophysiol 112:1729–1745.

Thatcher RW, North D, Biver C (2005): EEG and intelligence: relations between EEG coherence, EEG phase delay and power. Clin Neurophysiol 116:2129–2141.

Varela FJ, Toro A, John ER, Schwartz EL (1981): Perceptual framing and cortical alpha rhythm. Neuropsychologia 19:675–686.

Velleman P (1997): Datadesk Statistical Program, v. 6.0. Ithaca, NY: Data Description.

von Stein A, Sarnththeim J (2000): Different frequencies for different scales of cortical integration: from local gamma to long range alpha/theta synchronization. Int J Psychophysiol 38:301–313.

Yarowsky P, Kadekaro M, Sokoloff L (1983): Frequency dependent activation of glucose utilization in the superior cervical ganglion by electrical stimulation of cervical sympathetic trunk. Proc Natl Adad Sci U S A 80:4179–4183.

Yarowsky P, Crane A, Sokoloff L (1985): Metabolic activation of specific postsynaptic elements in superior cervical ganglion by antidromic stimulation of external carotid nerve. Brain Res 334: 330–334.